HHS Public Access

Author manuscript

Microsc Res Tech. Author manuscript; available in PMC 2023 October 01.

Published in final edited form as:

Microsc Res Tech. 2021 December ; 84(12): 2968–2976. doi:10.1002/jemt.23856.

Evaluation of enhanced darkfield microscopy and hyperspectral imaging for rapid screening of TiO_2 and SiO_2 nanoscale particles captured on filter media

Nicole M. Neu-Baker[1], **Alan K. Dozier**[2], **Adrienne C. Eastlake**[2], **Sara A. Brenner**[1,3]

[1]College of Nanoscale Science & Engineering, Nanobioscience Constellation, State University of New York (SUNY) Polytechnic Institute, Albany, New York, USA

[2]National Institute for Occupational Safety and Health (NIOSH), Cincinnati, Ohio, USA

[3]United States Food and Drug Administration (FDA), Office of In Vitro Diagnostics and Radiological Health, Office of Product Evaluation and Quality, Silver Spring, Maryland, USA

Abstract

Here we report on initial efforts to evaluate enhanced darkfield microscopy (EDFM) and light scattering Vis–NIR hyperspectral imaging (HSI) as a rapid screening tool for the offline analysis of mixed cellulose ester (MCE) filter media used to collect airborne nanoparticulate from work environments. For this study, the materials of interest were nanoscale titanium dioxide (TiO_2) and silicon dioxide (SiO_2; silica), chosen for their frequent use in consumer products. TiO_2 and SiO_2 nanoscale particles (NPs) were collected on MCE filter media and were imaged and analyzed via EDFM-HSI. When visualized by EDFM, TiO_2 and SiO_2 NPs were readily apparent as bright spherical structures against a dark background. Moreover, TiO_2 and SiO_2 NPs were identified in hyperspectral images. EDFM-HSI images and data were compared to scanning transmission electron microscopy (STEM), a NIST-traceable technique for particle size analysis, and the current gold standard for offline analysis of filter media. As expected, STEM provided more accurate sizing and morphology data when compared to EDFM-HSI, but is not ideal for rapid screening of the presence of NPs of interest since it is a costly, low-throughput technique. In this study, we demonstrate the utility of EDFM-HSI in rapidly visualizing and identifying TiO_2 and SiO_2 NPs on MCE filters. This screening method may prove useful in expediting time-to-knowledge compared to electron microscopy. Future work will expand this evaluation to other industrially relevant NPs, other filter media types, and real-world filter samples from occupational exposure assessments.

Correspondence: Nicole M. Neu-Baker, College of Nanoscale Science, Nanobioscience Constellation, State University of New York (SUNY) Polytechnic Institute, 257 Fuller Road, Albany, NY, 12203, USA. nneu@sunypoly.edu.

CONFLICT OF INTEREST

The authors declare no potential conflict of interest.

DISCLAIMER

The findings and conclusions in this report are those of the authors and do not necessarily represent the official position of the National Institute for Occupational Safety and Health, Centers for Disease Control and Prevention. Mention of any company or product does not constitute endorsement by the National Institute for Occupational Safety and Health, Centers for Disease Control and Prevention.

SUPPORTING INFORMATION

Additional supporting information may be found online in the Supporting Information section at the end of this article.

Keywords

mixed cellulose ester; occupational exposure assessment; pixel classification; reference spectral library; spectral angle mapper

1 | INTRODUCTION

As industries are increasingly incorporating engineered nanomaterials (ENMs) into their products and manufacturing processes, workers may be exposed via inhalation to ENMs when handling, processing, or disposing these materials in the workplace. The National Institute for Occupational Safety and Health (NIOSH) recommends decreasing the potential for exposure to ENMs, like carbon nanotubes or nanoscale titanium dioxide, because studies identify these materials as having the potential to impact work-related respiratory diseases (US CDC-NIOSH, 2009 “Respiratory Diseases”; US CDC-NIOSH, 2007). Occupational exposure assessments are critical for the monitoring and characterization of potential exposures to hazardous materials or materials of unknown toxicity in order to protect worker health and safety. Current NIOSH ENM exposure assessment methodology includes collection of airborne ENMs onto filter media (Eastlake et al., 2016; Methner, Hodson, Dames, & Geraci, 2010; Methner, Hodson, & Geraci, 2010) for offline direct visualization via transmission electron microscopy (TEM) for particle sizing, count, and morphology, typically coupled with energy-dispersive x-ray spectroscopy (EDS) for compositional analysis. The current TEM-EDS methods for carbon nanotubes (CNTs) and/or carbon nanofibers (CNFs) collected on filter media are based on methods for micron-sized asbestos (ASTM, 2003; US CDC-NIOSH, 1994), which may not be appropriate for analysis of ENMs. Furthermore, TEM-EDS is low-throughput, expensive, and time- and resource-intensive. Sample preparation is non-trivial and analysis requires highly-skilled microscopists. These limitations, in addition to the limited number of commercial labs with such capacity to perform modified TEM methods for ENMs, make this modality impractical for industrial occupational exposure assessment, routine monitoring, or any type of high-throughput analysis. In reality, many samples obtained in workplace settings may not contain ENMs in appreciable number, making routine TEM a time-intensive undertaking; therefore, in routine air sampling, even for tasks of high priority, it would be ideal to have a faster, less expensive screening modality available. Enhanced darkfield microscopy (EDFM) and hyperspectral imaging (HSI) are poised to fill that role.

HSI is an established technique for large-scale applications, including remote sensing, geospatial analysis, and food safety (Gowen, O’Donnell, Cullen, Downey, & Frias, 2007; Manolakis, Marden, & Shaw, 2003; van der Meer et al., 2012). More recently, it has been applied to the analysis of nanoscale materials (Roth, Tahiliani, Neu-Baker, & Brenner, 2015). The combined EDFM and light scattering Vis–NIR HSI CytoViva system (CytoViva, Inc., Auburn, AL) uses oblique angle illumination to detect scattered light in the sample, thereby easily visualizing nanoscale particles (NPs) as small as approximately 15 nm with high signal-to-noise in a variety of biological and environmental matrices. Using spectrophotometry and advanced optics and algorithms, a spectrum (400–1,000 nm) is captured from each pixel in a hyperspectral image. Spectral profiles for known NPs are

collected into reference spectral libraries (RSLs), which are used to identify those NPs in other samples (Roth, Sosa Peña, Neu-Baker, Tahiliani, & Brenner, 2015; Sosa Peña et al., 2016). Pixel classification algorithms, such as the spectral angle mapper (SAM), are used in conjunction with an RSL to classify pixels in hyperspectral images as NP(+) or NP(−), thereby providing data regarding particle composition and abundance. Note that since EDFM-HSI does not have sufficiently high resolution to determine if a single pixel represents a single particle or an aggregate or agglomerate of multiple smaller particles, we cannot say that an NP(+) pixel equals one nanoparticle. Therefore, we refer to NP(+) pixels as "structures" instead.

Here, we explore the application of this imaging and characterization modality for the analysis of titanium dioxide (TiO_2) and silicon dioxide (silica; SiO_2) NPs collected on mixed cellulose ester (MCE) filter media. These materials were chosen since TiO_2 and SiO_2 NPs are industrially relevant materials that are incorporated into numerous consumer products, and MCE filter media is commonly used to sample airborne nanoparticulate from industrial work environments. Previous work included the development of a sample preparation technique for EDFM-HSI analysis of MCE filter media (Neu-Baker, Eastlake, & Brenner, 2019). If EDFM-HSI proves to be a useful rapid screening technique, it will expedite data collection and analysis as well as the implementation of worker safety protocols, if warranted.

2 | MATERIALS & METHODS

2.1 | Sample generation

MCE filters were exposed to TiO_2 and SiO_2 NPs with loading masses that span the RELs for each material.

2.1.1 | TiO_2 NPs on MCE filters—MCE filters were exposed to TiO_2 NPs (20–40 nm diameter; AER-OXIDE P 25, Fisher Scientific, Fair Lawn, NJ). An aerosol of TiO_2 was created via an acoustic aerosol generation system (NIOSH HELD, Morgantown, WV) (McKinney, Chen, & Frazer, 2009; McKinney, Chen, Schwegler-Berry, & Frazer, 2013) using Leland pumps to create samples at a flow rate of 4 LPM with loading concentrations of 10.4 mg (22 s), 19.4 mg (43 s), and 32.8 mg (86 s). Filter blanks were prepared using filtered air only. An $n = 3$ per exposure group was prepared and analyzed, with an $n = 2$ prepared and analyzed for filter blanks. Filters at the highest loading concentration (32.8 mg) were used as positive controls.

2.1.2 | SiO_2 NPs on MCE filters—An aerosol of SiO_2 NPs (10–20 nm particle size; Sigma Aldrich, St. Louis, MO) was created via a Venturi aerosolization system (NIOSH DART; Cincinnati, OH) (Evans, Turkevich, Roettgers, Deye, & Baron, 2013). SiO_2 powder is placed into an exterior holding tube attached to the holding chamber. Air is pulled through the holding tube at a given volumetric flow rate ($Q = 60$ L/min), resulting in a flow rate of approximately 70 m/s. The aerosolized product in the chamber is then pulled through two different filter samples onto 37 mm diameter MCE filters. One sample is pulled through a cyclone and the other through a closed-face cassette and collected simultaneously (4 min). Filters exposed to loading masses of 3.0 mg, 2.0 mg, or 1.5 mg SiO_2 NPs ($n = 4$ for 1.5 mg;

n = 5 for 2.0 mg and 3.0 mg) were analyzed in this study. Blank filter samples (n = 2) were collected using the Venturi system, but without introduction of product into the chamber. Pre- and post-sampling filter weights were obtained.

2.2 | Sample preparation for microscopy

Exposed MCE filters were prepared for EDFM-HSI following the method published by Neu-Baker et al. (2019). A portion of each filter (approximately 20–25% of the filter) was cut with a clean scalpel and placed on a cleanroom-cleaned glass microscopy slide (NEXTERION, SCHOTT North America, Inc., Tempe, AZ). A cleanroom-cleaned glass coverslip (NEXTERION) was placed on top of the filter but was not adhered. Acetone (approximately 500 μl) was pipetted in between the slide and coverslip to saturate the filter and render it transparent. The coverslip was then sealed with clear nail polish.

2.3 | Enhanced darkfield microscopy (EDFM) and hyperspectral imaging (HSI)

Optical darkfield (DF) images and hyperspectral datacubes—hyperspectral images containing spatial and spectral data—were captured as previously described (Dillon, Bezerra, del Sosa Pena, Neu-Baker, & Brenner, 2017; Idelchik et al., 2016; Roth, Sosa Peña, et al., 2015; Sosa Peña et al., 2016). Briefly, DF images and hyperspectral datacubes were obtained with a 40× air objective to optimize the number of structures in a given field of view (FOV) and to expedite time-to-knowledge. Note, as mentioned, we use the term “structures” to indicate individual particles and/or aggregates or agglomerates of multiple particles since the resolution of EDFM-HIS is not high enough to differentiate. Datacubes were captured using standard low spatial resolution (2 × 2 pixel binning), giving a pixel size of 322.5 nm. The CytoViva HSI system (CytoViva, Inc., Auburn, AL) is capable of detecting structures smaller than the pixel size (particles ≥15 nm diameter) due to light scatter. Ten DF images and 10 corresponding datacubes per sample were captured in areas where TiO_2 or SiO_2 NPs were seen as bright spots against a dark background. DF images and hyperspectral datacubes were also collected for filter blanks. DF images were captured with gain of 0 dB and shutter of 10 ms for the TiO_2 samples and gain of 2.4–5.9 dB and shutter of 50–64 ms for the SiO_2 samples. Hyperspectral datacubes were captured with an exposure time of 0.05 s for the TiO_2 samples and an exposure time of 0.1–0.25 s for the SiO_2 samples to ensure the spectral intensity of the pixels did not exceed the maximum intensity of the system [16,000 arbitrary units (AU)]. DF images and hyperspectral datacubes were collected with a lamp source brightness of 60% for the TiO_2 samples and 75% for the SiO_2 samples. This discrepancy is due to the difference in amount of light scattering by the samples: the TiO_2 NPs appeared brighter in DF due to greater light scattering compared to the SiO_2 NPs, so the lamp source brightness was therefore reduced for the TiO_2 samples. All datacubes were corrected for contributions of the halogen light source. Following correction for the light source, all datacubes were spectrally subset from 450–725 nm to remove noise at <450 nm and >725 nm that could interfere with hyperspectral classification analysis.

2.4 | Creation of reference spectral libraries (RSLs)

Reference spectral libraries (RSLs) were created following methods presented by Roth, Sosa Peña, et al. (2015). The particle filtering method in the ENVI 4.8 (Harris Geospatial Solutions, custom for Cyto-Viva, Inc.) HSI software was used to collect spectra from pixels

associated with TiO_2 and SiO_2 NPs from lamp-corrected and subset datacubes of positive control samples (32.8 mg for TiO_2 and 3 mg for SiO_2) based on spectral intensity (>3,000 AU or at least twice the intensity of background pixels) and particle size (particles >80 pixels were excluded as they were visually determined likely to correspond to filter debris). The spectra identified by particle filtering from each of the positive controls were combined into one preliminary spectral library (SL) for each NP type. Each SL was then filtered against two datacubes of filter blanks to remove duplicative spectra from the SLs that are associated with the filter and/or potential contamination from the exposure process. The filtered SLs were considered the final RSLs for mapping and NP identification

2.5 | Pixel classification and identification of TiO_2 and SiO_2 NPs

The spectral angle mapper (SAM) algorithm in the ENVI 4.8 HSI software was used to classify pixels in the hyperspectral datacubes as NP(+) or NP(—). The default SAM threshold (0.10 rad) was used. SAM compares the spectrum of each pixel in a datacube to all spectra in the RSL. A positive match between the pixel spectrum and the RSL results in the classification of that pixel as NP(+). A mapped image is created with a false coloration overlay corresponding to NP(+) and NP(—) pixels, indicating the presence and location of TiO_2 or SiO_2 NPs in the sample based on SAM results. Relative abundance of NP(+) pixels are based on class distribution results from SAM, which generates the number and percentage of classified versus unclassified pixels.

2.6 | High angle scanning transmission electron microscopy (STEM) darkfield imaging with energy dispersive x-ray spectroscopy (EDS)

The existing method for electron microscopy of filter media—NIOSH Method 7402 (US CDC-NIOSH, 1994)—is strictly applicable to asbestos fibers. The method was later modified for fibrous carbonaceous nanomaterials, such as nanotubes and nanofibers. Neither the original method nor the modified version can be applied to this sample set since the TiO_2 particles of interest can be as small as 10 nm, requiring a magnification of 40,000× or higher to make them distinguishable from other background particles or contaminants. Unlike the TiO_2 filter samples, the SiO_2 filter samples had very low extraneous background particles. Thus, the SiO_2 particles could be easily identified by their near-spherical or agglomerated morphology. Consequently, a procedure was developed for the analysis of very small particles on MCE filter media. TEM sample grids were prepared using a common dimethylformamide (DMF) dissolution technique (US CDC-NIOSH, 1994) after carbon coating and collapsing the MCE filters. Scanning transmission electron microscopy (STEM) darkfield imaging was used to visualize the smallest particles while scanning the sample at 40,000–60,000× magnification. In STEM mode, they are easily visible without the use of a high contrast charged couple device (CCD) camera in TEM mode. The darkfield detector was used with auto-contrast turned off and a contrast setting applied such that a particle would saturate the image, making the particles easy to identify while scanning. A brightfield detector was used in conjunction with the darkfield detector with auto-contrast turned on, allowing for an unsaturated image of the whole field to be seen while scanning. The other advantage to doing the scanning in STEM mode is that it allows the microscopist to quickly increase magnification to perform energy dispersive x-ray spectroscopy (EDS) on small particles without needing to converge the beam, change spot size, and readjust the beam

position, as would be the case in TEM mode. The microscopist is therefore able to very efficiently switch between observation and analysis, which is particularly important when the particles of interest are only a small fraction of the total. However, because of the high magnifications used to count and measure the smaller particles using the STEM, a much smaller area was scanned as compared to the HSI samples. The average area scanned using the STEM was .023 mm^2 whereas the average area scanned per sample using HSI was 1.123 mm^2. Thus, the STEM counts would have much poorer counting statistics as compared to HSI.

3 | RESULTS

3.1 | Imaging of NPs via EDFM

Preparation of MCE filter samples for imaging was simple and quick, following the recently published protocol (Neu-Baker et al., 2019). Image capture via EDFM was likewise simple and quick, with TiO_2 and SiO_2 NPs readily apparent as bright spherical structures against a dark background at all loading concentrations (Figure 1). No TiO_2 or SiO_2 NPs were apparent in filter blanks (Figure 1). It is important to note that, although the TiO_2 and SiO_2 filters were generated using two different laboratory techniques, it does not affect imaging or hyperspectral data, since the generation methods do not transform the NPs in any way.

3.2 | Classification of spectral data

RSLs were created from datacubes of positive control samples (3.0 mg SiO_2; 32.8 mg TiO_2; Figure 2) and used with the SAM algorithm to classify pixels as NP(+) in datacubes of filters at all loading concentrations for both NP types (Figure 3). Since the datacubes were first normalized for the contributions of the light source, the RSLs are therefore also normalized and can be used for MCE filter media exposed to TiO_2 or SiO_2 NPs. Pixels classified as TiO_2(+) are indicated by a green false coloration overlay while pixels classified as SiO_2(+) are indicated by an aqua false coloration overlay. For comparison, spectral intensity of background or blank filters are typically between 0 and 2,000 AU (data not shown) (Neu-Baker et al., 2019), whereas the spectra for SiO_2 and TiO_2 have intensities of up to 40,000 AU.

3.3 | STEM-EDS

Typical grid openings of MCE filter backgrounds from the TiO_2 sample set were uniformly covered with background particles consisting of aluminum oxide, calcium, and bismuth. The TiO_2 particles ranged in size from 10 nm–20 μm. No TiO_2 structures were observed in the MCE filter blank (vehicle control). Select STEM images are shown in Figure 4. A plot of TiO_2 structure count is shown in Figure 5. Lower magnification STEM images are shown in Figure S1 for comparison to HSI datacubes.

3.4 | Comparison of EDFM-HSI and STEM-EDS

Comparisons of EDFM-HSI and STEM-EDS in identifying and approximating particle counts for SiO_2 and TiO_2 are shown in Figures 5 and 6. The number of pixels classified as TiO_2(+) (Figure 5, left) and SiO_2(+) (Figure 6, left), based on comparison to the respective RSLs, show a direct relationship between NP(+) pixels and the loading mass for both

materials. However, it is important to note the variability in the data, particularly for TiO_2 (Figure 5). Similar trends were seen for STEM (Figures 5, right and 6, right), but the considerable variability limits the conclusions that can be drawn from this data. It is also important to note that the HSI pixel counts and STEM structure counts cannot be directly compared to each other, as the resolution of HSI prohibits discrimination between individual NPs and agglomerates. Rather, the plots show the considerable variability in the counts, regardless of imaging modality, driven by particle agglomeration and small sample sizes. Furthermore, as previously mentioned, the area scanned per sample by HSI is considerably larger than the area scanned by STEM (1.123 mm^2 and 0.023 mm^2, respectively).

4 | DISCUSSION

This work represents the initial evaluation of EDFM-HSI as a potential screening tool for the rapid direct visualization and assessment of ENMs captured on filter media from occupational exposure assessments. The primary advantages of this imaging and ENM characterization modality over TEM/STEM—the current standard for direct visualization of ENMs captured on filters—are the considerable reduction in cost and time-to-knowledge (Sosa Peña et al., 2016). The sample preparation step (Neu-Baker et al., 2019) is appropriately quick and easy for a rapid screening protocol (one to 2 min per sample). Darkfield and hyperspectral imaging is also fast: darkfield images can be captured instantaneously after the FOV is identified; hyperspectral datacubes take longer to capture, around five to 10 min per FOV, on average, based on the settings used here (Neu-Baker et al., 2019). RSL creation can be tedious, requiring testing and refinement over several days or weeks, but this is a one-time initial step required for a new NP and/or filter media type (e.g., polycarbonate). Once the RSL is created, subsequent classification analysis is rapid (minutes per image). The potential time investment needed for RSL creation is not necessarily a hindrance to adoption of EDFM-HSI as a rapid screening method, unless new NPs and/or filter media types are frequently used. It should be emphasized that the TEM/STEM method is a hands-on process with each particle being analyzed by EDS and manually measured by the microscopist, whereas the EDFM-HSI method is an automated process that uses the SAM algorithm once the RSL is created. This makes the TEM/STEM method very inefficient when compared to the EDFM-HSI method, especially when analyzing particles down to the 10 nm size scale.

The comparison between EDFM-HSI and STEM performed here confirmed the known limitation that EDFM-HSI cannot compete with STEM in terms of resolution. Regardless, resolution may be sacrificed in favor of the speed of analysis associated with a screening technique. If higher resolution is desired for a particular sample to reveal more nuanced characterization data, such as structure concentration, particle size, morphology, or agglomeration, that sample may then move on to more intensive TEM/STEM analysis based on initial EDFM-HSI results. An intermediary step may be to collect hyperspectral datacubes at 100× magnification with high spatial resolution (1 × 1 pixel binning, creating 64 nm pixels); however, this may unnecessarily slow down a rapid screening protocol, especially for samples with low concentrations of ENMs, and would not provide considerably more data.

It is important to note the considerable variability in TiO_2 and SiO_2 structure counts by both HSI and STEM (Figures 5 and 6). The small sample size ($n = 3$ per exposure concentration for TiO_2 and $n = 4$ or 5 for SiO_2) is a very likely contributor to this variability. Further, the tendency of the TiO_2 NPs to agglomerate was likely the driving force behind the variability for that material, as the structure counts were based off the number of individual particles seen by STEM, regardless of whether they were isolated single particles or part of an agglomerate. Lower magnification STEM images and structure counts for TiO_2 and SiO_2 structures >500 nm are shown in Supplemental Information (Figures S1 and S2). Moreover, the size of the agglomerates was variable, with regard to the number of individual particles comprising the agglomerates. These are likely the factors also contributing to variability in NP(+) pixel count by HSI (Figures 5 and 6). A larger sample set would provide a better understanding of the particle count and distribution in the samples. This finding also serves as a limitation of EDFM-HSI: particle count may be underestimated by this method. However, if EDFM-HSI is simply used to ascertain presence or absence of the NP of interest, and is not used in any quantitative manner, as we suggest here, then the limitation becomes irrelevant. Estimates of particle or structure count may be instead determined by electron microscopy following initial screening by EDFM-HSI.

Additionally, STEM-EDS confirmed the important background cor rection step done when creating an RSL for HSI analysis: contaminant particles consisting of aluminum oxide, calcium, and bismuth were identified by STEM-EDS in filter blanks. By correcting for the background, any spectra associated with contaminant particles or the filter itself are removed from the library and do not become part of the RSL.

Here, we show that EDFM can easily visualize TiO_2 and SiO_2 NPs on filter media due to the light reflected by the particles and the high signal-to-noise of EDFM. Furthermore, we demonstrate that spectral data can be used to identify TiO_2 and SiO_2 NPs. It is important to note that this initial demonstration of this technique was done with lab-generated samples and do not reflect real-world samples collected from working environments that may also contain other materials or contaminants. Additional study using field-captured samples is needed for a more thorough evaluation of the utility of this technique as a screening tool. Initial investigations have indicated some overlap in the spectra in the RSLs for TiO_2 and SiO_2 (data not shown) and so it may not be possible to distinguish between the two materials in the event that they are co-contaminants in a real-world industrial setting. However, as a screening tool and from a public health perspective, it may be sufficient to identify metal oxides in general without needing more specificity. If needed, additional analysis via STEM could follow. Regardless, these initial results are promising. Based on the comparison to STEM, EDFM-HSI can provide limited data regarding TiO_2 and SiO_2 structure counts or agglomeration state and may thereby underestimate potential exposure. However, there is utility in a rapid screening method that simply generates “present/absent” qualitative data. Furthermore, EDFM-HSI may be an attractive in-house alternative to electron microscopy from a cost perspective, since ownership costs are far less than those for TEM (Sosa Peña et al., 2016). Additionally, EDFM-HSI allows for faster manual scanning at 10× magnification of a larger filter area (20–25% wedge of a 37 mm-diameter filter) than can be done with TEM, where sample sizes are restricted to 3 mm: this can be done in minutes at low 10×

magnification with EDFM-HSI, compared to weeks at “low” 1,000× magnification with TEM (Sosa Peña et al., 2016).

5| CONCLUSIONS

This work represents an initial investigation into the utility of EDFM-HSI as a rapid screening tool to expedite analysis of filter media. Here, we demonstrate that EDFM-HSI can easily visualize TiO_2 and SiO_2 NPs (>15 nm in size) captured on MCE filter media and, moreover, hyperspectral data can be used to locate and identify the NPs. While it cannot provide high-magnification, high-resolution images, details on particle agglomeration state or size, or a precise structure count, we show here that it can inform the researcher of the presence or absence of the material of interest in the absence of potential interfering contaminants, which is highly useful for a screening technique. If those additional details are needed, EDFM-HSI can eliminate the samples that do not have the material of interest, so that the intensive electron microscopy analysis is only carried out on the samples that are known to have the material of interest. EDFM-HSI is poised to serve as a screening tool for rapid assessments of potential NP exposure in work environments. Just as phase contrast microscopy (PCM) and polarized light microscopy (PLM) have been used to rapidly screen air filter samples for asbestos, EDFM-HSI can fill that role for ENMs that are non-fibrous and difficult or impossible to identify by PCM or PLM. In order to have a meaningful impact on exposure science for ENMs, this protocol should be expanded to include other industrially relevant ENMs, other filter media types (e.g., polycarbonate), and should ultimately be tested on real-world samples captured in work settings. At the current stage, this technique shows promise for eventual incorporation as a rapid screening tool into the larger scheme of exposure assessment methodology.

Supplementary Material

Refer to Web version on PubMed Central for supplementary material.

ACKNOWLEDGMENTS

This research effort was financially supported by the National Institute for Occupational Safety and Health (NIOSH). N.M. Neu-Baker received funding from NIOSH through Interagency Personnel Assignments (14IPA1418072 & 18IPA1816710-M03) and a contract (200-2017-M-94751). The authors thank CytoViva, Inc. (Auburn, AL) for technical support and guidance. Additionally, the authors thank Pramod Kulkarni, Sam Glover, and Paul Siegel (NIOSH) for review of this manuscript.

Funding information

National Institute for Occupational Safety and Health, Grant/Award Numbers: 14IPA1418072, 18IPA1816710-M03, 200-2017-M-94751

DATA AVAILABILITY STATEMENT

The data that support the findings of this study are available from the corresponding author upon reasonable request.

Abbreviations:

DF	darkfield
EDFM	enhanced darkfield microscopy
EDS	energy-dispersive x-ray spectroscopy
ENM	engineered nanomaterial
FOV	field of view
HSI	hyperspectral imaging
MCE	mixed cellulose ester
NP	nanoscale particles
PCM	phase contrast microscopy
PLM	polarized light microscopy
RSL	reference spectral library
SAM	spectral angle mapper
SL	spectral library
STEM	scanning transmission electron microscopy
TEM	transmission electron microscopy

REFERENCES

ASTM. (2003). D5755–03, Standard test method for microvacuum sampling and indirect analysis of dust by transmission electron microscopy for asbestos structure number surface loading West Conshohocken, PA: ASTM International.

Dillon JC, Bezerra L, del Sosa Pena MP, Neu-Baker NM, & Brenner SA (2017). Hyperspectral data influenced by sample matrix: The importance of building relevant reference spectral libraries to map materials of interest. Microscopy Research and Technique, 80, 462–470. [PubMed: 28139043]

Eastlake AC, Beaucham C, Martinez KF, Dahm MM, Sparks C, Hodson LL, & Geraci CL (2016). Refinement of the nanoparticle emission assessment technique into the nanomaterial exposure assessment technique (NEAT 2.0). Journal of Occupational and Environmental Hygiene, 13, 708–717. [PubMed: 27027845]

Evans DE, Turkevich LA, Roettgers CT, Deye GJ, & Baron PA (2013). Dustiness of fine and nanoscale powders. The Annals of Occupational Hygiene, 57, 261–277. [PubMed: 23065675]

Gowen AA, O'Donnell CP, Cullen PJ, Downey G, & Frias JM (2007). Hyperspectral imaging—an emerging process analytical tool for food quality and safety control. Trends in Food Science and Technology, 18, 590–598.

Idelchik M.d. P. S. , Neu-Baker NM, Chandrasekaran A, Friedman AJ, Frame MD, & Brenner SA (2016). Relative quantitation of metal oxide nanoparticles in a cutaneous exposure model using enhanced darkfield microscopy and hyperspectral mapping. NanoImpact, 3–4, 12–21.

Manolakis D, Marden D, & Shaw GA (2003). Hyperspectral image processing for automatic target detection applications. Lincoln Laboratory Journal, 14, 79–116.

McKinney W, Chen B, & Frazer D (2009). Computer controlled multi-walled carbon nanotube inhalation exposure system. Inhalation Toxicology, 21, 1053–1061. [PubMed: 19555230]

McKinney W, Chen B, Schwegler-Berry D, & Frazer DG (2013). Computer-automated silica aerosol generator and animal inhalation exposure system. Inhalation Toxicology, 25, 363–372. [PubMed: 23796015]

Methner M, Hodson L, & Geraci C (2010). Nanoparticle emission assessment technique (NEAT) for the identification and measurement of potential inhalation exposure to engineered nanomaterials—Part a. Journal of Occupational and Environmental Hygiene, 7, 127–132. [PubMed: 20017054]

Methner M, Hodson L, Dames A, & Geraci C (2010). Nanoparticle emission assessment technique (NEAT) for the identification and measurement of potential inhalation exposure to engineered nanomaterials—Part B: Results from 12 field studies. Journal of Occupational and Environmental Hygiene, 7, 163–176. [PubMed: 20063229]

Neu-Baker NM, Eastlake AC, & Brenner SA (2019). Sample preparation method for visualization of nanoparticulate captured on mixed cellulose ester filter media by enhanced darkfield microscopy and hyperspectral imaging. Microscopy Research and Technique, 82, 878–883. [PubMed: 30768825]

Roth GA, Sosa Peña M d. P., Neu-Baker, N. M., Tahiliani, S., & Brenner, S. A. (2015). Identification of metal oxide nanoparticles in histological samples by enhanced darkfield microscopy and hyperspectral mapping. Journal of Visualized Experiments, 106, e53317.

Roth GA, Tahiliani S, Neu-Baker NM, & Brenner SA (2015). Hyperspectral microscopy as an analytical tool for nanomaterials. Wiley Interdisciplinary Reviews: Nanomedicine Nanobiotechnology, 7, 565–579. [PubMed: 25611199]

Sosa Peña M.d. P. , Gottipati A, Tahiliani S, Neu-Baker NM, Frame MD, Friedman AJ, & Brenner SA (2016). Hyperspectral imaging of nanoparticles in biological samples: Simultaneous visualization and elemental identification. Microscopy Research and Technique, 79, 349–358. [PubMed: 26864497]

US CDC-NIOSH. (1994). National Institute for Occupational Safety and Health (NIOSH). U.S. Centers for Disease Control. NIOSH Manual of Analytical Methods (NMAM®) 4th edition (2014). Method 7402: Asbestos by TEM. Schlecht, P. C., O'Connor, PF. Available online at: http://www.cdc.gov/niosh/docs/2003-154/pdfs/7402.pdf.

US CDC-NIOSH. (2007). Progress toward safe nanotechnology in the workplace. DHHS (NIOSH) Publication No. 2007–123 Cincinnati, OH: National Institute for Occupational Safety and Health.

US CDC-NIOSH. (2009) Approaches to safe nanotechnology: managing the health and safety concerns associated with engineered nano materials. DHHS (NIOSH) Publication 2009–125 Cincinnati, OH: National Institute for Occupational Safety and Health; https://www.cdc.gov/niosh/docs/2009-125/pdfs/2009-125.pdf.

van der Meer FD, van der Werff HMA, van Ruitenbeek FJA, Hecker CA, Bakker WH, Noomen MF, … Woldai T (2012). Multi- and hyperspectral geologic remote sensing: A review. International Journal of Applied Earth Observation and Geoinformation, 14, 112–128.

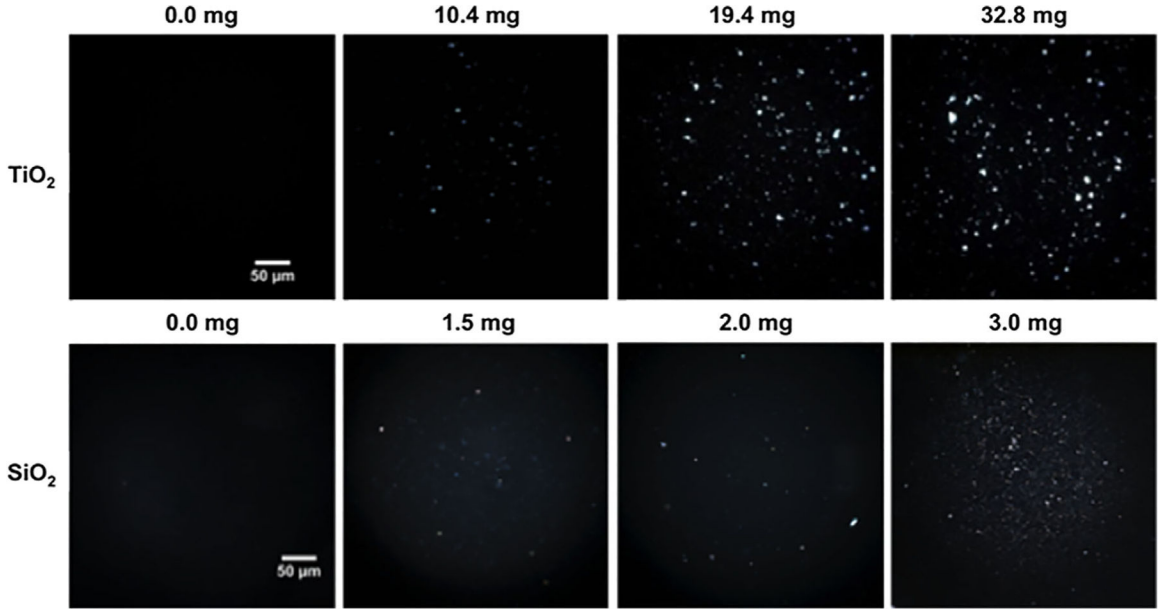

FIGURE 1.

Optical DF images of TiO_2 and SiO_2 NPs captured on MCE filter media. Optical images captured by EDFM of MCE filters exposed to TiO_2 NPs (top row) or SiO_2 NPs (bottom row). Top row, from left to right: filter blank exposed to filtered air only (TiO_2 NP exposure concentration of 0.0 mg); 10.4 mg TiO_2; 19.4 mg TiO_2; and 32.8 mg TiO_2. TiO_2 NPs are easily visible as bright white structures on a dark background. Scale bar = 50 μm. Bottom row, from left to right: filter blank exposed to filtered air only (SiO_2 NP exposure concentration of 0.0 mg); 1.5 mg SiO_2; 2.0 mg SiO_2; and 3.0 mg SiO_2. SiO_2 NPs are easily visible as bright white structures on a dark background. Scale bar = 50 μm [Color figure can be viewed at wileyonlinelibrary.com]

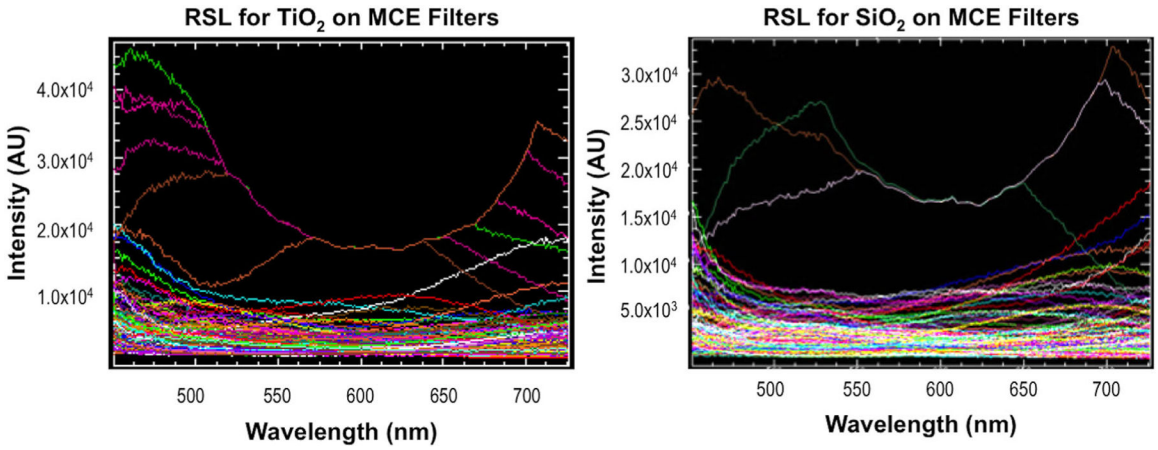

FIGURE 2.

Reference spectral libraries (RSLs) for TiO_2 and SiO_2 NPs on MCE filter media. RSLs containing spectra unique to pixels associated with TiO_2 NPs (left) and with SiO_2 NPs (right) were used to classify pixels in hyperspectral images as TiO_2 or $SiO_2(+)$ or TiO_2 or $SiO_2(-)$ using the spectral angle mapper (SAM) algorithm [Color figure can be viewed at wileyonlinelibrary.com]

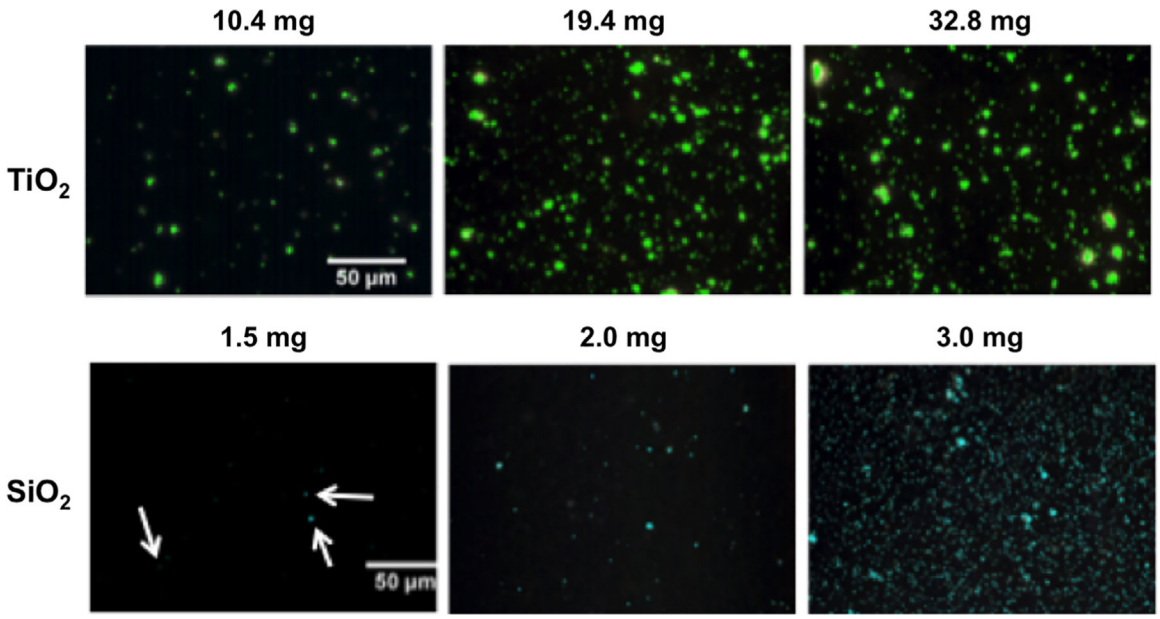

FIGURE 3.

Classified hyperspectral images of TiO_2 and SiO_2 NPs collected on MCE filter media. Hyperspectral datacubes of TiO_2 (top row) and SiO_2 NPs (bottom row) captured on MCE filter media. Top row, from left to right: 10.4 mg TiO_2 loading mass; 19.4 mg TiO_2; and 32.8 mg TiO_2. Green false coloration overlay indicates TiO_2(+) pixels as identified by SAM. Scale bars = 50 µm. Bottom row, from left to right: 1.5 mg SiO_2 loading mass; 2.0 mg SiO_2; and 3.0 mg SiO_2. Aqua false coloration overlay indicates SiO_2(+) pixels as identified by SAM. Scale bars = 50 µm. Pixels may represent single NPs or agglomerates [Color figure can be viewed at wileyonlinelibrary.com]

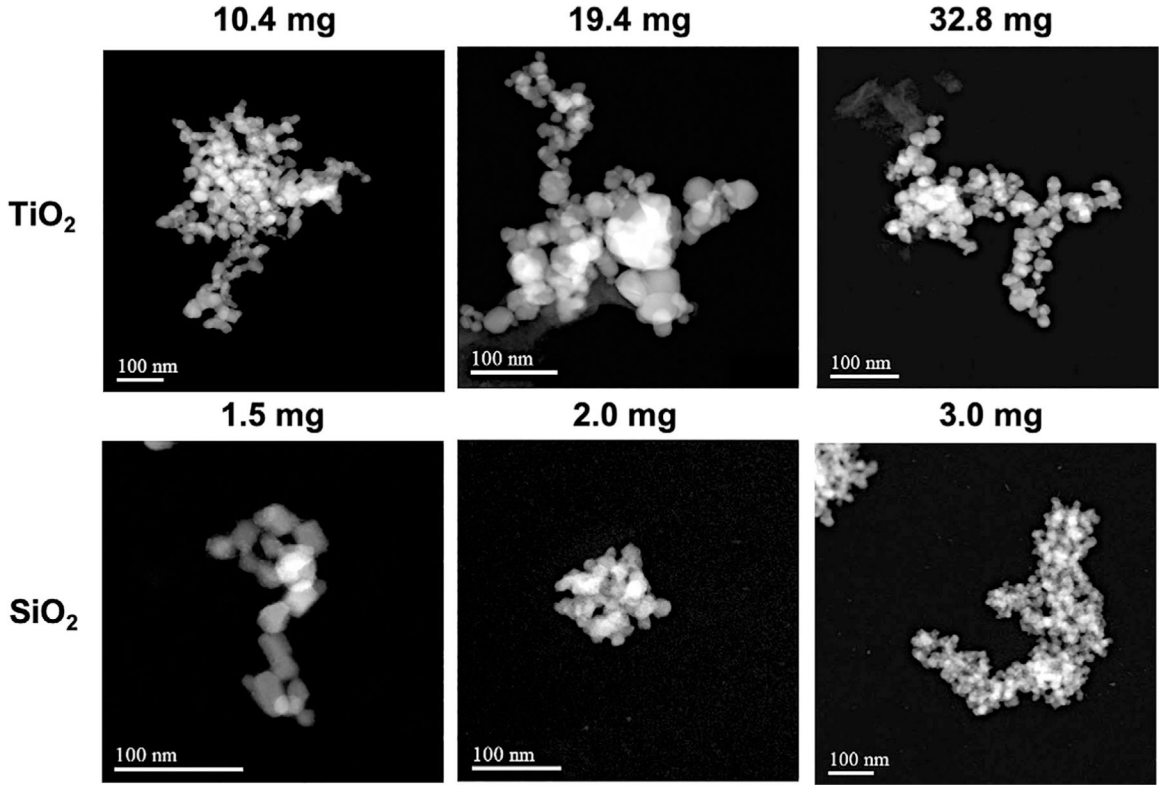

FIGURE 4.

STEM images of TiO_2 and SiO_2 NPs collected on MCE filter media. STEM images of TiO_2 and SiO_2 NPs captured on MCE filter media. Top, from left to right: representative filter samples exposed to 10.4 mg TiO_2; 19.4 mg TiO_2; and 32.8 mg TiO_2. TiO_2 NPs were typically seen as agglomerates and not as individual particles. Bottom, from left to right: representative filter samples exposed to 1.5 mg SiO_2; 2.0 mg SiO_2; and 3.0 mg SiO_2. Scale bars = 100 nm. SiO_2 NPs were typically seen as agglomerates and not as individual particles

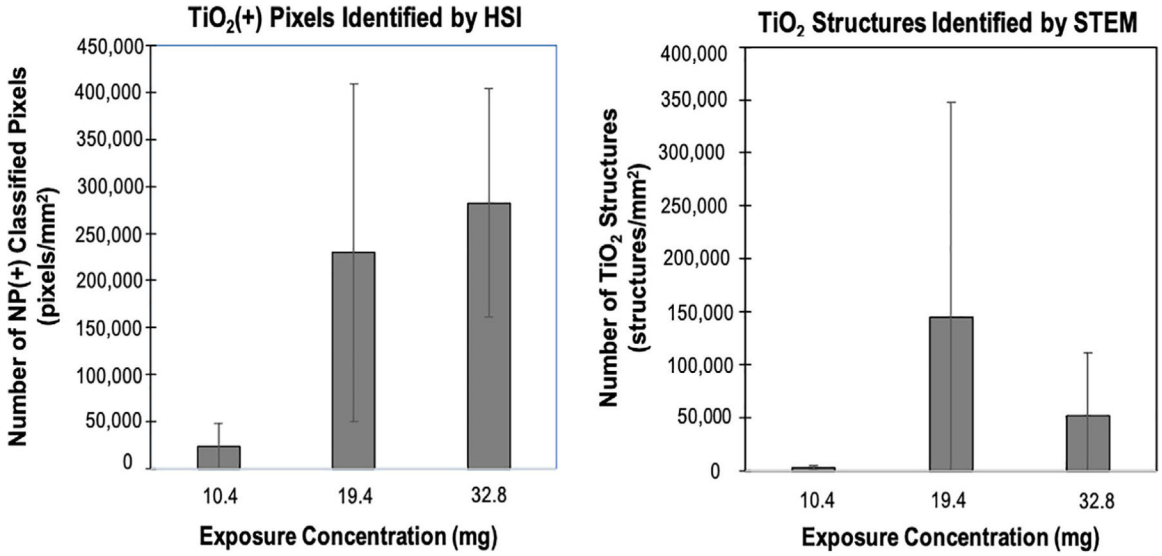

FIGURE 5.

TiO_2 comparison of HSI and STEM data. Left: plot shows the number of pixels classified as TiO_2(+) with HSI (as pixels/mm^2). Right: plot shows the TiO_2 structure count for each loading mass (as structures/mm^2). Error bars = ± 1 *SD* from the mean. $N = 3$ for each loading mass [Color figure can be viewed at wileyonlinelibrary.com]

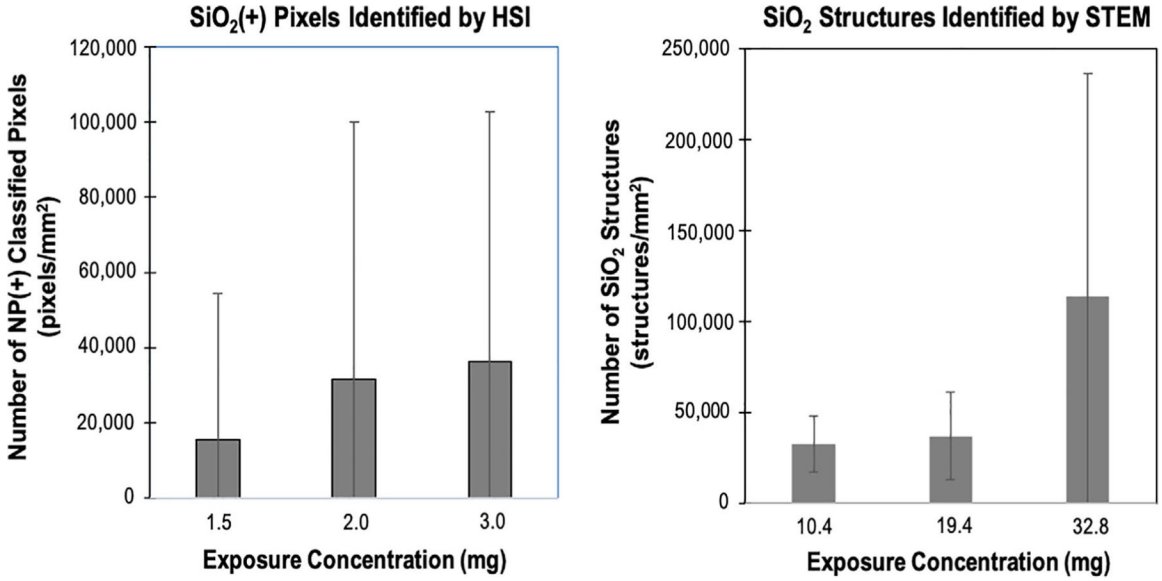

FIGURE 6.

SiO_2 comparison of HSI and STEM data. Left: plot shows the number of pixels classified as SiO_2(+) with HSI (as pixels/mm^2). Right: plot shows the SiO_2 structure count for each loading mass (as structures/mm^2). Error bars = ± 1 *SD* from the mean. $N = 4$ for 1.5 mg loading mass; $n = 5$ for both 2.0 mg and 3.0 mg loading mass [Color figure can be viewed at wileyonlinelibrary.com]